

Copyright 1998, Society of Photo-Optical Instrumentation Engineers

This paper was published in Optical Microlithography XI, Volume 3334 and is made available as an electronic reprint with permission of SPIE. One print or electronic copy may be made for personal use only. Systematic or multiple reproduction, distribution to multiple locations via electronic or other means, duplication of any material in this paper for a fee or for commercial purposes, or modification of the content of the paper are prohibited.

# Illumination pupil filtering using modified quadrupole apertures

Bruce W. Smith, Lena Zavyalova, John S. Petersen\*

Rochester Institute of Technology, 82 Lomb Memorial Dr., Rochester, N.Y. 14623, bwsemc@rit.edu

\*SEMATECH, 2706 Montopolis Dr., Austin, TX 78741, john.petersen@sematech.org

## ABSTRACT

Off-axis illumination schemes have been developed that can enhance both the resolution and focal depth performance for an optical exposure tool. One approach introduced modifies the illumination profile, filling the condenser lens pupil with weak gaussian quadrupoles where energy is distributed within and between poles. This method has demonstrated better control of DOF and proximity effect for a variety of feature types. Other possibilities also exist. Presented here are approaches to illumination modification through use of condenser lens masking apertures, fabricated as attenuating fused silica reticles which are inserted at the lens pupil plane. Application of this technique for use in high NA 248 nm and 193 nm exposure tools is shown. For each case, optimization of illumination profiles has been conducted. Optimized source files have been converted to halftone (dithered) masking files for electron beam patterning on fused silica with chromium and anti-reflective (AR) films. Analysis of these modified illumination techniques in terms of resolution, focal depth, throughput, and aberration performance is also presented.

## 1. INTRODUCTION

Off-axis illumination has the ability to significantly improve both the resolution and focal depth for a given optical lithographic technology. For dense features (with line-to-space duty ratios on the order of 1:1 to 1:3), analysis of such improvements can be quite straight forward. Performance improvements are realized when illumination is obliquely incident on a mask at an angle so that zeroth and first diffraction orders are distributed on alternative sides of the optical axis. These two diffraction orders are sufficient for imaging and it can be shown that the minimum pitch value for this oblique condition of partially coherent illumination  $\lambda/NA$ <sup>1</sup>. A significant impact of off-axis illumination is realized when considering focal depth. In the case of zero pole width, diffraction orders travel an identical path length regardless of the defocus amount. The consequence is a depth of focus which is effectively infinite. In practice, by limiting illumination to allow for one narrow beam or pair of beams leads to zero intensity. Also, imaging is limited to features oriented along one direction in an x-y plane. To overcome this, an annular or quadrupole configuration may be employed to deliver illumination at the angles needed with a finite distribution to allow for some finite intensity. Resulting focal depth is less than that for the ideal case but improvement over a full circular aperture can be achieved.

When considering isolated features, discrete diffraction orders do not exist but instead a continuous diffraction pattern is produced. Convolution of such a frequency representation with either illumination poles or annular rings will result in diffraction information distributed over a range of angles. Isolated line performance is therefore minimally effected by off-axis illumination. In the region where features are neither truly isolated nor dense (finite duty ratios greater than 1:3 for instance), the frequency separation of diffraction orders is small enough so that performance is not likely to be improved with off-axis illumination. Features of this type are generally considered to be isolated. When dense and isolated features exist together in a field, it follows that the dense to isolated feature size bias or proximity effect can be worsened by using off-axis illumination. Modifications to off-axis illumination has been introduced to alter the illumination beam profile<sup>2</sup>. This modified illumination approach fills the condenser lens pupil with gaussian poles (or weak quadrupoles), where energy is distributed within and between poles. The effective result is a combination of off-axis and on-axis illumination for best dense and isolated line performance respectively. This weak quadrupole illumination can also lead to improvements when used with weak phase-shift masking. When combined with attenuated phase shift masking, for instance, the increased distribution of energy over lens pupil serves to reduce the printability of side lobes<sup>3</sup>. The effect is similar to that for increasing partially coherence. In this case, however, enhancement remains from the off-axis component of illumination.

## 2. OPTIMIZING OFF-AXIS ILLUMINATION DESIGNS

### 2.1 STRONG QUADRUPOLE OPTIMIZATION

Uniform conventional illumination using circular apertures generally requires definition of the partial coherence factor ( $\sigma$ ). If uniform "top-hat" illumination does not exist, additional parameters may be required to describe the distribution of energy. In any case, first order optimization for a given geometry / wavelength / NA combination can be straight forward. When considering off-axis illumination, definition of several additional parameters is needed. An example will be used here to demonstrate the additional requirements needed when considering quadrupole illumination for a variety of duty ratios. In this case, 130 nm features have been targeted for imaging with a 193 nm exposure wavelength using an objective lens numerical aperture of 0.60. Duty ratios from 1:1 to 1: 6 are included. Features are considered dense with a duty ratio less than 1:3. Table 1 shows the pitch values (p) for these dense features along with the required axis center sigma and quadrupole center sigma ( $\sigma_c$ ) values for optimum off-axis illumination. Center sigma values on axis are determined as  $\lambda/(2p \cdot NA)$ , as shown in Figure 1. Since diffraction order placement is determined by the projection of the quadrupole onto the x or y axis, the center quadrupole sigma values are larger by a  $\sqrt{2}$  factor.

Duty	Pitch nm	axis sigma	quad sigma
1:1	260	0.61	0.87
1:1.5	325.00	0.50	0.71
1:2	390.00	0.42	0.59
1:2.5	455.00	0.35	0.49

**Table 1.** Pitch values and corresponding center sigma values for 130 nm features with 1:1 to 1:2.5 duty ratio.

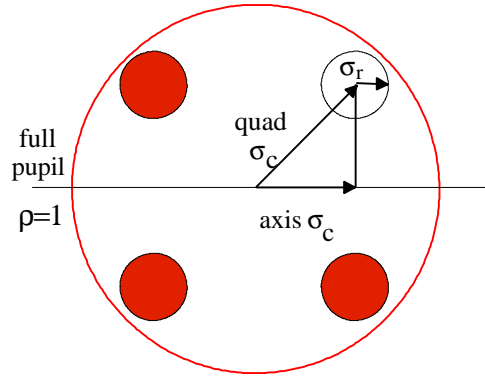


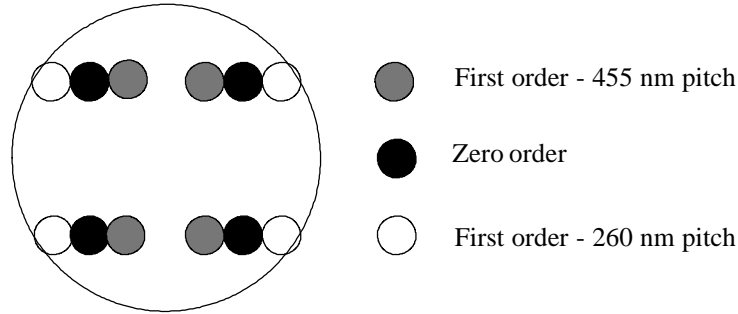
**Figure 1.** Schematic of quadrupole illumination, plotted in the frequency plane of the objective lens. The frequency distribution of zero and first diffraction orders coincide in the objective lens pupil when the axis center sigma ( $\sigma_c$ ) is chosen as  $\lambda/(2p \cdot NA)$ . The corresponding quadrupole  $\sigma_c$  is  $\sqrt{2} \lambda/(2p \cdot NA)$ , which limits the maximum  $\sigma_c$  to  $1/\sqrt{2}$ .

In order to design an off-axis illumination configuration that can accommodate and enhance the range of pitch values in Table 1, pole position and radius values must be chosen so that some amount of order overlap occurs for each case. This can be accomplished if the quadrupole center  $\sigma_c$  and the radius  $\sigma_r$  values are set as follows:

$$\sigma_c = \frac{\sqrt{2} (0.61 + 0.35)}{2} = 0.68$$

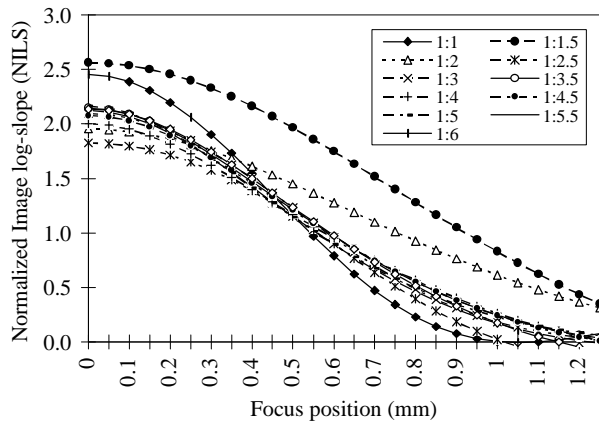
$$\sigma_r > \frac{0.61 - 0.35}{2} = 0.13$$

These choices for pole center and radius values correspond to the situation where zero and first diffraction orders begin to overlap for the extreme pitch values of 260 and 455 nm as shown in Figure 2. The  $\sqrt{2}$  term does not factor into determination of  $\sigma_r$  values since the pole radius is projected directly onto the axes. The extent of order overlap for these extreme pitch values is, however, mostly ineffectual and larger  $\sigma_r$  values are required to influence performance. A  $\sigma_r$  value of 0.20 allows for significant order overlap (~20%) and is a more practical starting value for further optimization.

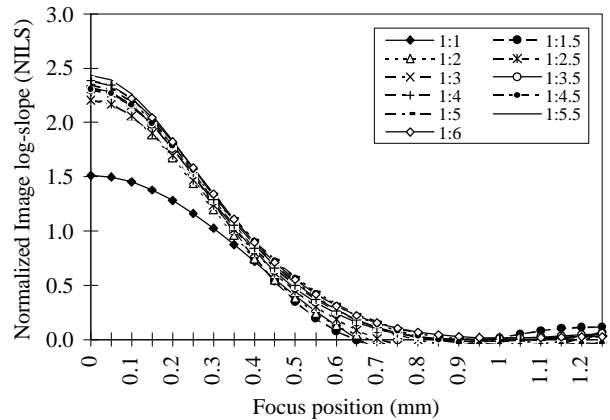


**Figure 2.** Diffraction orders (first and zero) for 130 nm x-oriented features using quadrupole illumination, plotted in the frequency plane of the objective lens. Center sigma is 0.68 and radius sigma is 0.13, chosen to accommodate feature pitch values from 260 to 455 nm.

To evaluate the performance improvement for these 130 nm feature, normalized aerial image log-slope NILS (normalized to the feature size) is plotted against focus position in Figures 3 and 4 for quadrupole and conventional illumination<sup>4</sup>. These plots show how 1:1, 1:1.5, and 1:2 duty ratio features with the quadrupole illumination possess superior through-focus NILS performance when compared to larger pitch features. The 1:1.5 ratio features are significantly enhanced, as predicted by the choice of pole parameters. When more isolated features are considered however (with duty ratios 1:3 and greater), conventional illumination (in this case with a partial coherence factor of 0.7) is preferred. The use of this condition of off-axis does nothing to enhance these pitch values as first and higher diffraction orders are distributed away from  $\sigma_c$  frequency positions. To accommodate such large pitch features, pole positions closer to the optical axis would be needed, a situation that begins to approximate on-axis illumination. When imaging of both dense and isolated features, illumination that resembles both the strong quadrupole and the conventional on-axis illumination may then be desirable. This leads to the notion of weak quadrupole illumination design.



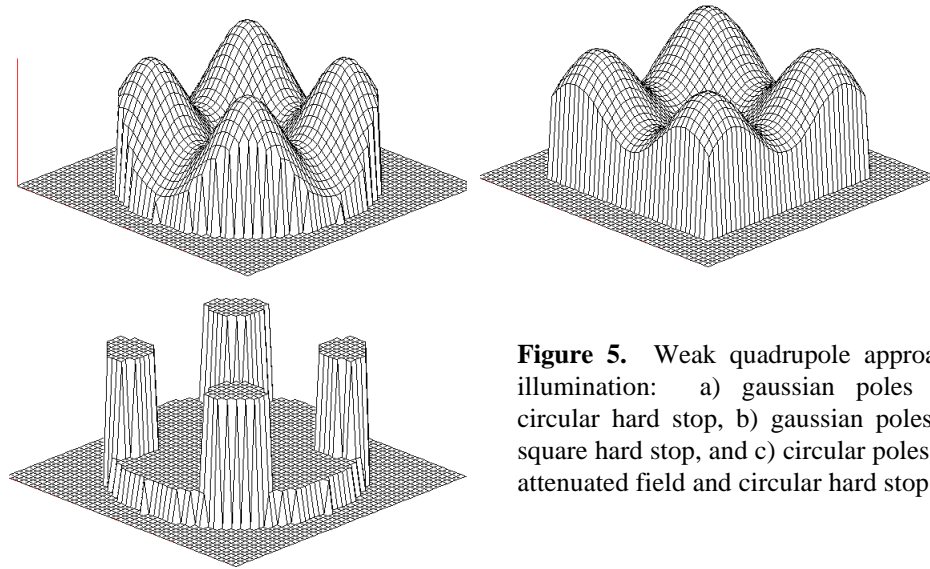
**Figure 3.** Normalized aerial image log-slope (NILS) vs focus for 130 nm features using quadrupole illumination,  $\sigma_c=0.68$  and  $\sigma_r=0.20$ .



**Figure 4.** Normalized aerial image log-slope (NILS) vs. focus for 130 nm features using conventional illumination,  $\sigma=0.70$ .

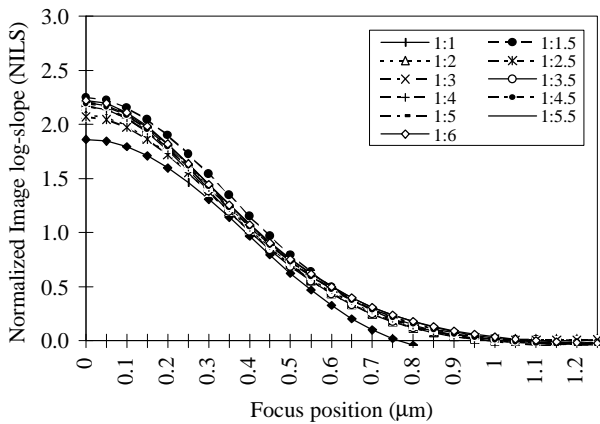
## 2.2 WEAK QUADRUPOLE OPTIMIZATION

Figure 5 shows three solutions for weak quadrupole illumination. The strong quadrupole design discussed previously was the starting point for each of these solutions. An on-axis component has been incorporated into each to allow for suitable imaging performance of the more isolated features. Figures 5a and 5b are diagrams of weak quadrupole illumination approaches using gaussian poles, where energy is distributed over the full pupil. A hard-stop is also used to limit the maximum on-axis conventional  $\sigma$  value. Figure 5a uses a circular aperture hard-stop while the approach shown in Figure 5b uses a square aperture. By using a square aperture, the on-axis, partially coherent diffraction order spread which contributes to modulation loss can be limited while the off-axis order overlap is retained. This superior solution is appropriate for x/y feature orientation only, which is most often encountered with IC microlithography. Figure 5c shows a weak quadrupole illumination approach that leads to similar solution by adding a conventional, on-axis component to illumination via an attenuated field or background. A background field intensity is chosen to be close the center intensity of the gaussian weak quadrupole approach for similar performance.



**Figure 5.** Weak quadrupole approaches to illumination: a) gaussian poles with a circular hard stop, b) gaussian poles with a square hard stop, and c) circular poles with an attenuated field and circular hard stop.

Figures 6 through 8 show NILS vs. defocus plots for imaging of 130 nm features using these three approaches. For each case, a center sigma value of 0.68 has been used. A gaussian pole width ( $\sigma_r$ ) of 0.30 leads to best NILS performance through focus and through pitch for designs corresponding to Figures 5a and 5b (gaussian designs). The optimum NILS



**Figure 6.** NILS vs. focus for 130 nm features using weak gaussian quadrupole illumination ( $\sigma_c=0.68$  and  $\sigma_r=0.30$ ) and a circular hard stop ( $\sigma=0.8$ ).

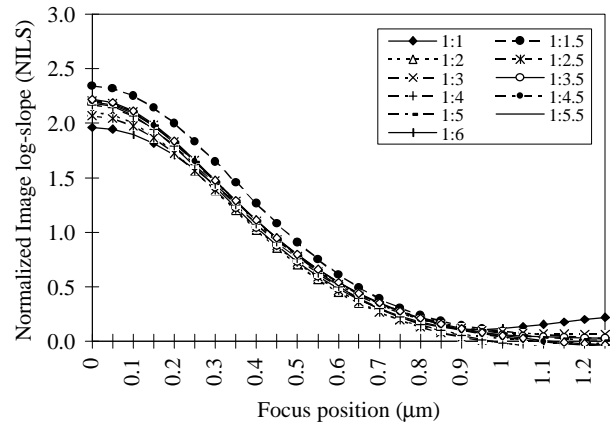


**Figure 7.** NILS vs. focus for 130 nm features using weak gaussian quadrupole illumination ( $\sigma_c=0.68$  and  $\sigma_r=0.30$ ) and a square hard stop (half-width =0.8).

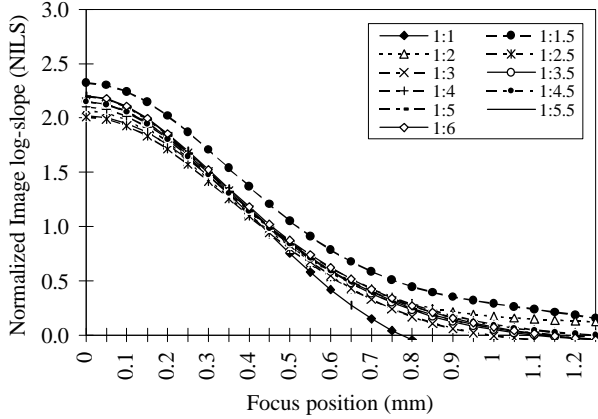


**Figure 8.** NLS vs. focus for 130 nm features using weak quadrupole illumination with top-hat, circular poles ( $\sigma_c=0.68$  and  $\sigma_f=0.20$ ), a circular hard stop ( $\sigma=0.8$ ), and a background intensity of 25%.

performance for the attenuated field design is achieved with  $\sigma_f=0.2$  and a background field intensity of 25%. The performance measured by image log-slope for all three cases is similar. There is, however, some performance gain for the square hard stop case which cannot be matched with any circular hard stop. A small increase in the pole size ( $\sigma_p$ ) for the attenuated field design can also lead to performance which matches more closely to the gaussian approaches. Other performance comparisons need to be made, including evaluation of throughput and aberration, before any one of these three approaches can be considered superior.

### 2.3 IMPACT ON THROUGHPUT

Exposure time is one component of exposure tool throughput. Table 2 is a comparison of the throughput efficiency of several variations of the weak quadrupole approach, measured relative to conventional illumination with a  $\sigma$  of 0.7. The worst case throughput is for the attenuated field design, where the total intensity through the pupil is 52% of that for conventional illumination with  $\sigma=0.7$ . The gaussian weak quadrupole approach with a  $0.7\sigma$  circular hard stop leads to 83% throughput and the same design with a  $0.7$  half-width square hard stop results in 85% throughput. If the square hard stop is increased in size to  $0.8$  half-width, the throughput increases to 93% and imaging performance remains comparable to the circular hard stop. This efficiency comes about because of the amount of energy allowed at the corners of the square pupil, where the diagonal approaches the full extent of the condenser lens pupil, or a  $\sigma$  value near 1.0. Comparison of intensity throughput is an important one as illumination modification is considered. If the illumination system of an exposure tool can allow full value,  $\sigma=1$  operation, this square hard stop variation of the weak quadrupole can lead to minimal losses.

Weak quadrupole design	Relative intensity
Conventional, $0.7\sigma$	1.00
Attenuated field, $0.68\sigma_c$ , $0.2\sigma_f$ , $0.8\sigma$ stop, 25% field	0.52
Weak gaussian, $0.68\sigma_c$ , $0.3\sigma_f$ , $0.7\sigma$ circular stop	0.83
Weak gaussian, $0.68\sigma_c$ , $0.3\sigma_f$ , $0.7\sigma$ square stop	0.85
Weak gaussian, $0.68\sigma_c$ , $0.3\sigma_f$ , $0.8\sigma$ square stop	0.93

**Table 2.** Comparison of weak quadrupole throughput

### 2.4 IMPACT ON ABERRATIONS

Optical lens aberration are most often evaluated for systems using the full extent of a circular pupil. As off-axis approaches are considered (such as the quadrupole approach explored here), the imaging characteristics of optical systems where the exit pupil is not completely utilized must be considered. The impacts of off-axis illumination on objective lens aberrations can be described in terms of an expanded set of polynomials which are orthogonal over appropriate regions of the pupil<sup>5</sup>. These polynomials can be derived from the Zernike circle polynomials<sup>6</sup> and describe the behavior of aberrations up to the sixth order ( $R_6^1$ ). Derivation is based on the distribution of diffraction information of dense features

when optimally illuminated off-axis. In this case, less than the entire lens pupil is utilized and instead only a radial portion determined by center and radii sigma is needed. The result is a set of two limiting terms: the inner portion of the objective lens pupil,  $\epsilon_1$ , and the outer portion of the pupil,  $\epsilon_2$ . The situation is depicted in Figure 9.

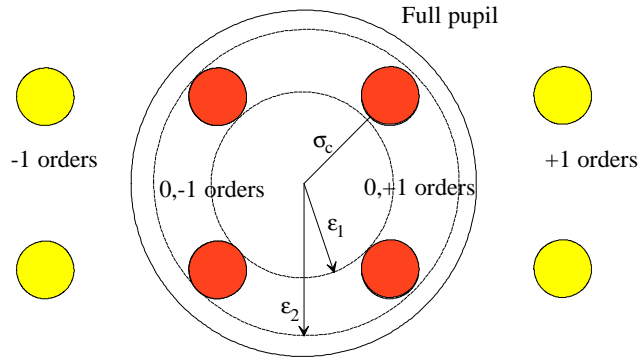


**Figure 9.** Diagram of the utilization of the objective lens pupil with quadrupole illumination.

For quadrupole illumination, these parameters are determined as:

$$\begin{aligned} \sigma_c &= (\epsilon_1 + \epsilon_2) / 2 \\ \sigma_r &= (\epsilon_1 - \epsilon_2) / 2 \end{aligned}$$

Insight into the influence that the use of specific pupil positions has on aberration can be gained by considering Figure 10. Shown here are wavefront deformation plots (as optical path deviation, OPD) for primary aberrations: coma, defocus, astigmatism, and spherical. Radially symmetric aberrations (spherical and defocus) will be improved as poles are moved off-axis and as pole size decreases. Coma and astigmatism (and also tilt) are not symmetric and can be made worse with

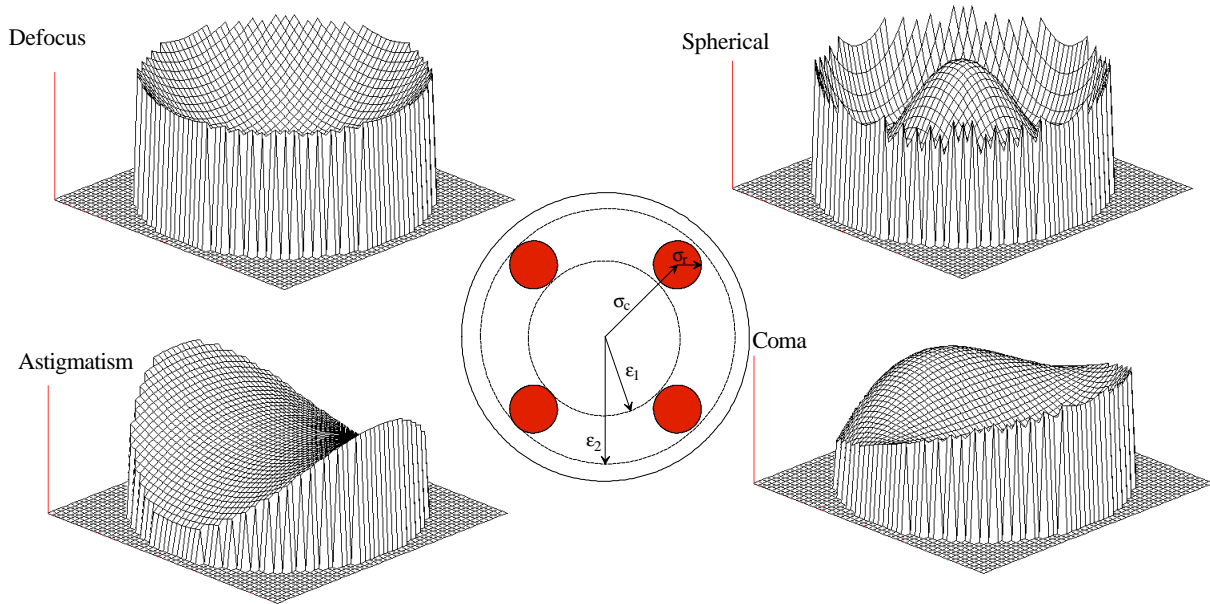


**Figure 10.** Wavefront deformation plots for primary aberrations and the portion of the lens pupil used with quadrupole illumination.

off-axis illumination. Measurement of the variance or standard deviation of phase error across the lens pupil allows for evaluation. Table 3 gives the form as well as the standard deviation (s) for balanced primary aberrations. The  $A_i$  term represents the peak value of an aberration. The form of each aberration is described as a phase error  $\Phi(r,\theta)$  and the standard deviation of balanced aberrations with  $\epsilon_1$  and  $\epsilon_2$ . Figures 11 through 15 show the standard deviation of each balanced aberration, plotted against  $\epsilon_1$  and  $\epsilon_2$ . In each case,  $\epsilon_1$  is plotted from 0 to 1.0 and  $\epsilon_2$  is plotted from 0.2 to 1.0 (x and y scales are normalized). No solution exists of course where  $\epsilon_1$  is greater than  $\epsilon_2$ . As predicted from Figure 10, off-axis illumination impacts symmetrical aberrations by decreasing their contribution. Astigmatism, coma, and tilt can be made worse. Coma, however, can be improved if it is appropriately balanced with wavefront tilt. In practical application, an increase in coma may be experienced since balancing is most likely performed for the full pupil.

Aberration	Phase aberration $\Phi(r,\theta)$	Standard deviation of phase aberration (s) / $A_i$
<i>Spherical</i>	$Z_9 [r^4 - (1 + \epsilon_1) r^2]$	$\frac{\sqrt{5}}{30} \sqrt{16\epsilon_2^4 - 2\epsilon_1^2\epsilon_2^2 - 30\epsilon_2^2 + 15 + \epsilon_2^4} (\epsilon_2 - \epsilon_1)(\epsilon_2 + \epsilon_1)$
<i>Coma</i>	$Z_{7,8} [r^3 - 2r/3(1+\epsilon_1^2+\epsilon_1^4)(1+\epsilon_1)]\cos\theta$	
<i>Astigmatism</i>	$Z_{5,6} [r^2(\cos^2\theta-1/2)]$	$\frac{\sqrt{6}}{12} \sqrt{\epsilon_2^4 + \epsilon_1^2 + \epsilon_1^4}$
<i>Defocus</i>	$Z_4 [r^2]$	$\frac{\sqrt{3}}{6} \sqrt{\epsilon_1^4 - 2\epsilon_1^2\epsilon_2^2 + \epsilon_2^4}$
<i>Tilt</i>	$Z_{2,3} [r\cos\theta]$	$\frac{1}{2} \sqrt{\epsilon_2^2 + \epsilon_1^2}$

**Table 3.** Description of balanced primary aberrations and corresponding standard deviations determined by quadrupole parameters.

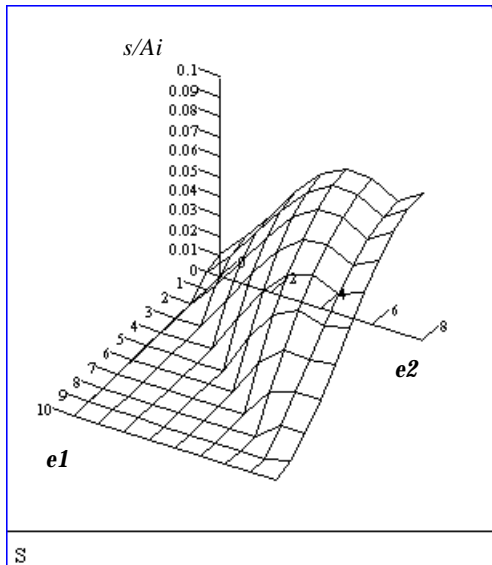


**Figure 11.** The standard deviation of balanced spherical aberration ( $Z_9$ ) normalized to the peak value ( $A_s$ ).

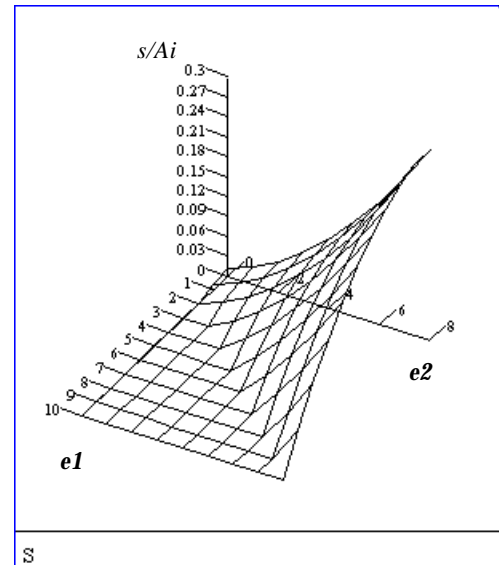


**Figure 12.** The standard deviation of defocus aberration ( $Z_4$ ) normalized to the peak value ( $A_d$ ).

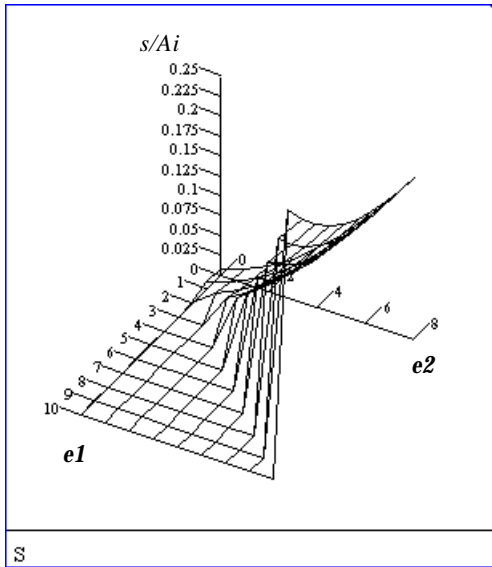


**Figure 13.** The standard deviation of balanced astigmatism aberration (Z5,6) normalized to the peak value (A<sub>a</sub>).

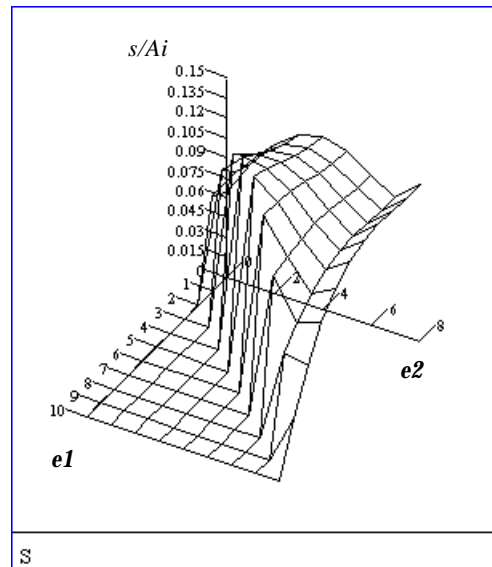


**Figure 14.** The standard deviation of balanced coma aberration (Z7,8) normalized to the peak value (A<sub>c</sub>).

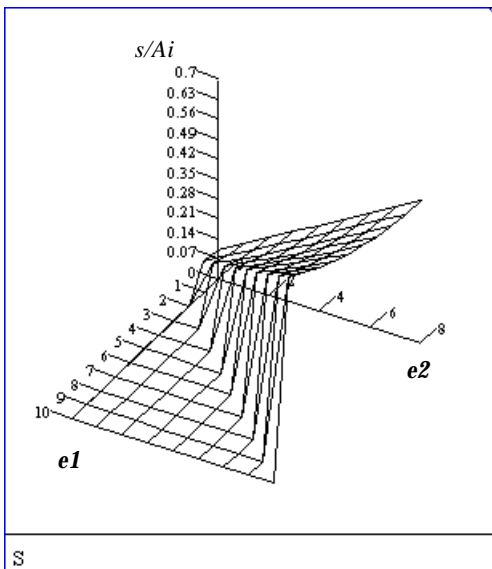


**Figure 15.** The standard deviation of wavefront tilt (Z2,3) normalized to the peak value (A<sub>t</sub>).

Although off-axis illumination can lead to improved performance through the reduction of some lens aberration, this may not necessarily be desirable when various feature types, masking levels, and illumination approaches are considered together. The influence of off-axis illumination on lens aberration can be minimized through the incorporation of some on-axis illumination component to more uniformly fill the lens pupil. This can be accomplished by using techniques such as the weak quadrupole approaches investigated here. It can be expected that the averaging effects of the approaches which reduce performance differences between dense and isolated features through focus will behave similarly with aberration.

### 3. FABRICATION AND IMPLEMENTATION OF APERTURES

Implementation of modifications to existing illumination system can be challenging but is possible if the condenser lens pupil is accessible. The approach utilized here involves the use of condenser lens masking apertures, fabricated as attenuating fused silica reticles, inserted at the lens pupil plane. Apertures have been fabricated for an ISI 248nm full field stepper, an ISI Microstep 193nm system, and an ASML 248 nm stepper. For each case, optimization of illumination profiles has been conducted via lithographic simulation (using Prolith/2) as described earlier. The resulting illumination profiles were then dithered and translated into a format compatible with a mask writing tool (MEBES format), resulting in a pixilated half-tone illumination file. Fused silica plates, 20 ml thick and sized appropriately for condenser pupil requirements, were coated (via sputtering) with  $\sim 1000\text{\AA}$  of a chromium film and a chromium oxide AR layer for reflectivity below 10% at 248 and 193 nm. A novolac-based resist (OCG 895i) was spin coated over the metal film stack and exposed at 10keV using a MEBES system with a 0.25  $\mu\text{m}$  beam width. Resist development (in 0.21N TMAH) and wet etch (in ceric ammonium nitride) followed and fused silica apertures were cut to appropriate sizes. Each exposure tool studied allowed access to the condenser pupil plane and custom fixturing was fabricated to accommodate the fused silica apertures. Alignment of apertures was made possible by incorporating alignment fiducials on the masking apertures and on the aperture holders. Table 4 contains a summary of apertures fabricated for 248 and 193nm.

Exposure tool	Design	Features optimized <sup>†</sup>
ISI 248nm / 0.53NA / 0.74 $\sigma_{\text{max}}$	Weak gaussian 0.68/0.3	0.18 to 0.22 $\mu\text{m}$
	Strong quadrupole 0.68/0.2	"
	Attenuated field 0.68/0.2/25%	"
	Conventional 0.7 sigma	"
ISI 193nm / 0.60NA / 1.0 $\sigma_{\text{max}}$	Weak quadrupole 0.7/0.15	0.12 to 0.16 $\mu\text{m}$
	Weak quadrupole 0.7/0.3*	0.10 to 0.18
	Weak quadrupole 0.8/0.3*	0.09 to 0.15
	Weak quadrupole 0.95/0.35*	0.08 to 0.13
ASML 248nm / 0.5NA / 0.68 $\sigma_{\text{max}}$	Strong quadrupole 0.65/0.2	0.19 to 0.22 $\mu\text{m}$
	Weak quadrupole 0.65/0.3	0.19 to 0.22
	Weak quadrupole 0.60/0.2	0.20 to 0.23
	Weak quadrupole 0.55/0.2	0.22 to 0.25

**Table 4.** Summary of apertures fabricated for 248 and 193nm exposure tools. \*Apertures have been reduced from a full  $\sigma=1$  using physical hard stops. <sup>†</sup>Specific feature sizes and pitch values are targeted by using circular and square hard stops.

### 4. EXPOSURE RESULTS

Results from exposures using the 193nm apertures listed in Table 6 are presented here. Exposures were performed with a small field ISI exposure tool operating at 0.6NA. A single layer chemically amplified resist was coated at thickness near 3000 $\text{\AA}$  over a 248nm organic ARC. Nominal exposure ranged from 12 to 15  $\text{mJ}/\text{cm}^2$ . Resist was developed in a TMAH developer. A series of resist exposures was conducted to generate focus / exposure matrices for each illumination condition using a binary chromium mask containing dense and isolated features to 0.10  $\mu\text{m}$ . Focus and exposure latitude results were compared to those using conventional illumination and a partial coherence factor of 0.7. Evaluation using a KLA 8100 top-down CD SEM allowed for estimation of depth of focus (DOF). Results are summarized in Table 7. Estimation of DOF values included criteria for feature clearing (without scum) and dense to isolated feature biasing. DOF values are given for nominal exposure with a +/- 10% exposure latitude window. Results for the weak quadrupole aperture with 0.7  $\sigma_c$  and 0.15  $\sigma_r$  resemble results expected for strong quadrupole illumination. The central intensity for this design is near zero and there is little distribution of energy outside of the central pole region.

Illumination condition	Resist features		
	0.12 $\mu\text{m}$	0.13 $\mu\text{m}$	0.14 $\mu\text{m}$
Conventional, $0.7 \sigma$	scum	0.10 $\mu\text{m}$	0.20 $\mu\text{m}$
Weak quad. $0.7\sigma_c/0.15\sigma_r$	scum	0.30 $\mu\text{m}$ (w/large bias)	0.45 $\mu\text{m}$ (w/large bias)
Weak quad. $0.7\sigma_c/0.3\sigma_r/0.8$ stop	scum	0.20 $\mu\text{m}$	0.40
Weak quad. $0.95\sigma_c/0.35\sigma_r$	0.25 $\mu\text{m}$	0.30 $\mu\text{m}$	0.35 $\mu\text{m}$

**Table 7.** DOF results from resist imaging results using various illumination conditions (193 nm 0.6NA, with a single layer chemically amplified resist coated near 3000Å over a 248nm organic ARC).

Although a significant improvement in DOF for dense features is experienced, a large dense to isolated feature bias results. The weak quadrupole illumination with  $0.7 \sigma_c$  and  $0.30 \sigma_r$  results in less DOF improvement than the  $0.15 \sigma_r$  case, as anticipated, but there is significant reduction in biasing between dense and isolated features. The  $0.95 \sigma_c$  and  $0.35 \sigma_r$  is an extreme case of the quadrupole design, where poles are pushed toward the edge of the condenser lens pupil (which is possible with in this case since the maximum conventional  $\sigma$  for this exposure tool is 1.0). Performance improvements are realized for 0.12 an 0.13  $\mu\text{m}$  features, as seen from Table 7 and also shown with SEM micrographs in Figure 16. Although modulation of features has been demonstrated down to 0.10 $\mu\text{m}$ , no usable DOF was achieved, due in part to adverse resist/ARC interaction effects.

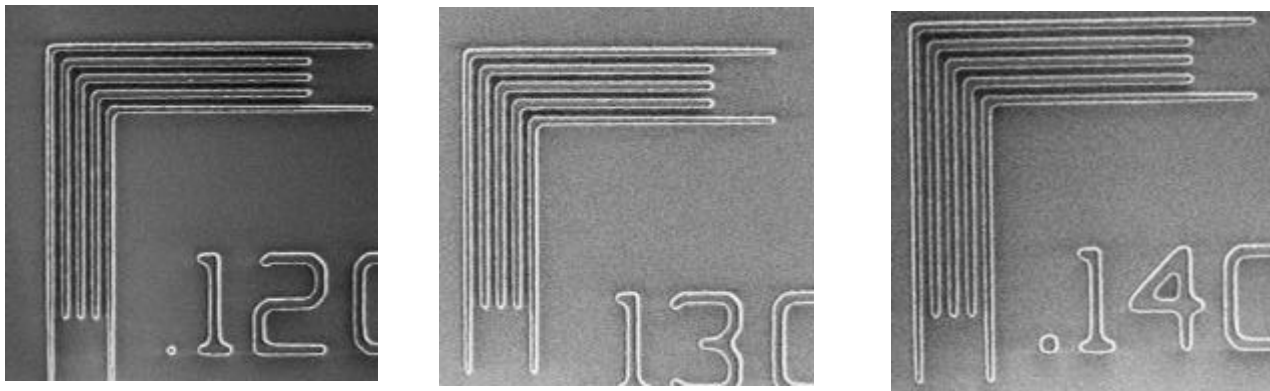


**Figure 16.** SEM micrograph of 0.12 to 0.14  $\mu\text{m}$  features imaged with a weak quadrupole aperture with  $0.95 \sigma_c$  and  $0.35 \sigma_r$ . Estimated usable DOF for each is 0.25  $\mu\text{m}$ , 0.30  $\mu\text{m}$ , and 0.35  $\mu\text{m}$  for 0.12  $\mu\text{m}$ , 0.13  $\mu\text{m}$ , and 0.14  $\mu\text{m}$  features respectively.

## 5. PUSHING THE LIMITS

The quadrupole approach to off-axis illumination is limited to features with pitch values of  $0.5 \sqrt{2} \lambda/\text{NA}$ . Two pole (dipole) off-axis illumination can offer resolution improvements over quadrupole. Pitch is not limited by projection of poles onto the x and y axes and values to  $0.5\lambda/\text{NA}$  can be achieved. To accommodate features of various duty ratios, an on-axis pole could be incorporated, sized appropriately for isolated features, resulting in a tri-pole design. This scheme is, however, limited to features in one direction only. An alternative approach is the cross-quadrupole off-axis design depicted in Figure 17. This cross-orientation is inherently weaker than the diagonal orientation because of the non-optimal or on-axis illumination component which is provided by poles that are not off-axis for a given feature orientation. This off-axis / on-axis approach is similar to the design goals for the weak quadrupole schemes discussed above. The benefit to using this method of off-axis illumination is that pitch values can be pushed  $\sqrt{2}$  further than with the diagonal approach,

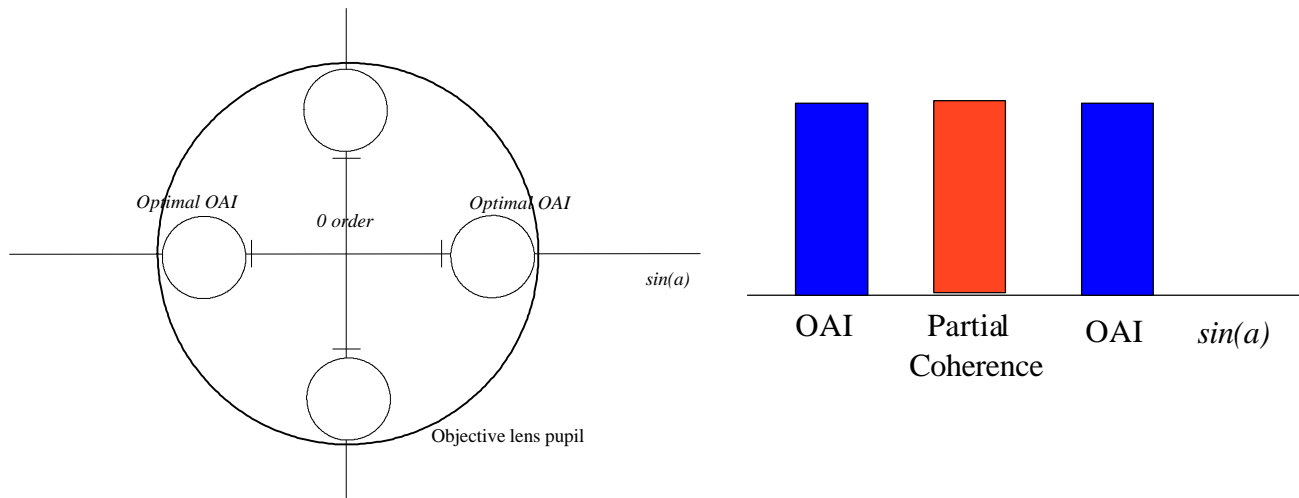


**Figure 17.** Schematic of the cross-quadrupole approach to weak off-axis illumination. For features oriented along one x or y direction, two poles deliver off-axis illumination while remaining poles deliver an on-axis component. The diagram on the right shows how x-oriented features experience both off-axis and on-axis (partially coherent) illumination.

allowing for dense/equal  $k_1$  values to 0.25 vs. 0.35 for the diagonal approach. Although imaging performance (measured by image log-slope for instance) can be closely matched across a large range of duty ratios using such weak cross-quadrupole designs, the overall image modulation is poor and additional methods of image enhancement would likely be required. By using such combined enhancement schemes, along with a suitably capable resist and process, dense feature resolution at or below 80 nm may be possible with a 193nm exposure wavelength.

## 6. CONCLUSIONS

An approach to implement off-axis, weak quadrupole illumination into existing exposure tools has been demonstrated. Several alternatives have been presented which lead to improvements in resolution, focal depth, and bias effects through a large range of feature duty ratios. A number of critical issues need to be considered as these enhancement techniques are employed. To be considered production worthy, intensity throughput needs to remain high. Additionally, the impact on aberrations becomes critical as the full objective lens pupil may no longer be fully utilized. The gaussian quadrupole technique of weak off-axis illumination, especially when combined with a square hard stop, has been shown here to be a robust approach in terms of imaging performance, throughput, and aberration tolerance. Implementation of such modifications to illumination has been demonstrated by fabricating pixilated, AR chrome on fused silica apertures using electron beam mask writing strategies. Apertures are inserted and aligned in the pupil plane of the condenser lens. Results show strong correlation to predicted performance in terms of resolution and focal depth improvement over a range of pitch values. This method of illumination control is not necessarily limited to quadrupole designs. Annulus apertures or more arbitrary designs (optimized for specific feature performance) could easily be incorporated. These approaches can also be applied to the majority of optical exposure tools existing today.

## 7. REFERENCES

- 1 B.W. Smith, Revalidation of the Rayleigh resolution and DOF limits, Proc. SPIE Vol. 3334 (1998).
- 2 T. Ogawa, M. Uematsu, T. Ishimaru, M. Kimura, T. Tsumori, Proc. SPIE Vol. 2197: 19 (1994).
- 3 B.W. Smith, S. Butt, Microlithography World, Summer 1997.
- 4 Simulations performed using Prolith/2 version 5.1.
- 5 B.W. Smith, J.S. Petersen, to be published.
- 6 F. Zernike, Physica, 1 (1934), 689.